Electron distribution function in the external corona of laser generated plasma

M. Mašek, K. Rohlena

Institute of Physics, ASCR, Na Slovance 2, 182 21 Prague 8, Czech Republic

Vlasov equation with a small collision term was solved simultaneously with the set of Maxwell equations in a 1D approximation to describe the phase space evolution of the electron distribution function corresponding to the outer corona of a nanosecond laser generated plasma. The decay of the heating laser wave in the back-scattered Raman wave and an electrostatic daughter wave is observed. The electrostatic wave is trapping the plasma electrons and shapes the electron distribution function. Later we observe wave cascading, frequency shift and intermittency.

1. Introduction

The physical situation in which an intense laser beam interacts with a developed plasma is met mostly in the direct drive compression experiments when a spherical target (capsule filled with a frozen D-T mixture on the inner wall) is illuminated by a system of laser beam, an outstreaming plasma is created and the rest of the laser pulse is interacting with this developed plasma plume. In the indirect drive experiments, the capsule is enclosed in a hohlraum, whose inner walls are again illuminated by the primary laser beams filling the inner space with an x-ray radiation absorbed by the capsule and causing its compression, [1]. The interaction then takes place near the light entrance holes, which let the beams inside the hohlraum.

The mechanism of laser plasma generation and heating by the impinging laser beam occurs mostly by the way of oscillatory motion of electrons in the electric field of the light wave, which is damped by the electron-ion collisions, dissipating thus the energy of the coherent laser wave, so called inverse bremsstrahlung mechanism. However, in the external part of the corona the laser plasma is, only weakly collisional and the evolution of the electron distribution function in the electron phase space is far from remaining a maxwellian one. The predominant mechanism causing deviations from a Maxwell distribution is the particle trapping in electrostatic waves. The electrostatic waves turn up in the plasma as daughter wave in the nonlinear processes of wave transformations, the typical example of which is the Raman scattering when the heating laser wave decays in a back-scattered electromagnetic wave and a forward directed electrostatic electron plasma wave. The potential troughs of this electrostatic wave are trapping the electrons which travel at nearly the same speed as the wave phase velocity and later start to oscillate around the wave potential minima. The oscillating electrons have their own dynamics separate from that of the bulk thermal electrons, which gives rise to additional wave modes. One of them is the trapped particle instability, which broadens the electrostatic spectrum and leads to an intermittency. The electron phase space is hardly accessible to a direct measurement of the electron distribution function, which is changing fast on a ps time scale, it therefore makes sense to resort to a numerical modeling of the phase space evolution. This is effected by a solution of the Vlasov equation (including a weak collision term) simultaneously with the Maxwell equations in a 1D periodic slab model by a transform method. The parameters of the computation were chosen to be compatible with the plasma in the laser corona typically generated by the nanosecond PALS system (Research centre PALS, Institute of Physics & Institute of Plasma Physics of ASCR) at the high flux end attainable by a tight focusing $\sim 10^{16}\mathrm{W/cm}^2$.

The importance of the electron phase space phenomena for the laser energy deposition to the target consists in the danger of hot electron production by insufficient laser energy dissipation in a collisionless plasma. The electron trapping may lead to electron acceleration by which a population of hot electrons is created. This may cause a target pre-heat and the compression will be impaired in the direct drive configuration. In the indirect drive the wave transformation is a more important phenomenon. The hohlraum is filled with the plasma having weak density gradients, which is prone to be Raman unstable, and at the
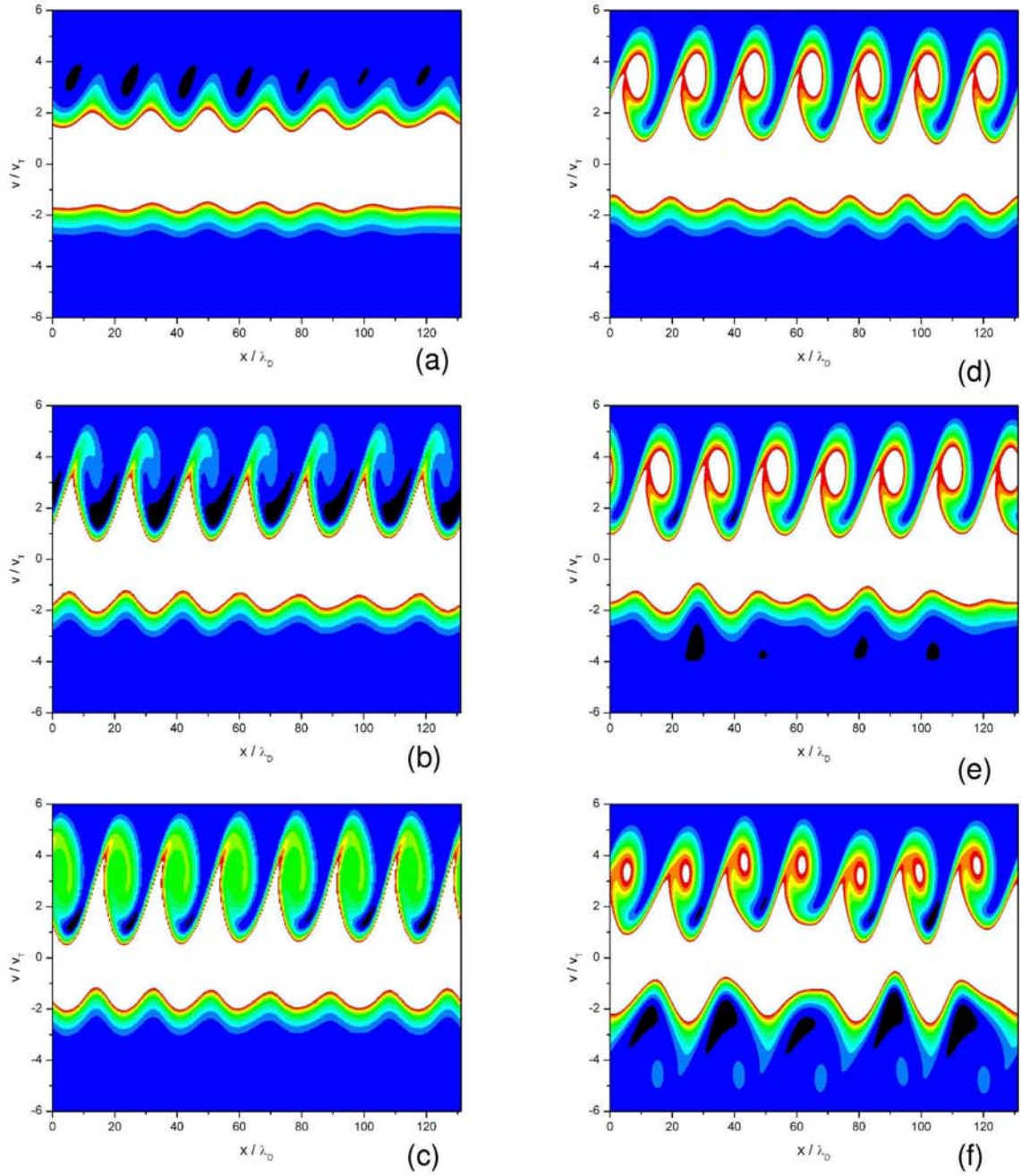
Figure 1: Phase-space contour plot of electron distribution function evolution at times (a) $\omega_{pe}t = 100$ (b) $\omega_{pe}t = 120$ (c) $\omega_{pe}t = 140$ (d) $\omega_{pe}t = 500$ (e) $\omega_{pe}t = 750$ (f) $\omega_{pe}t = 1100$. A linear scale of contour plots is used and the values of distribution function are in the interval between $f = 0.0$ and $f = 0.1$.

light entrance holes an intense Raman scattering may reflect a large portion of the incoming laser energy. The non-linear saturation of the Raman instability and the reflection coefficients are again largely dependent on the state of the electron distribution function. These phenomena became particularly important with the arrival of large projects like NIF and Megajoule, [2].

2. The fundamental system

In a 1D model we re-write the Vlasov equation and the Maxwell equations as

$$\frac{\partial f}{\partial t} + v_x \frac{\partial f}{\partial x} + \frac{e}{m}\left(\frac{\partial \varphi}{\partial x} - \frac{e}{m}A\frac{\partial A}{\partial x}\right)\frac{\partial f}{\partial v} = \quad (1)$$

$$= \nu_c\left(\frac{\partial(vf)}{\partial v} + <v^2> \frac{\partial^2 f}{\partial v^2}\right),$$

$$\left[\frac{\partial^2}{\partial x^2} - \frac{1}{c^2}\frac{\partial^2}{\partial t^2} - \frac{\omega_{pe}^2}{c^2}\frac{n_e}{n_0}\right]A = 0, \quad (2)$$

$$\frac{\partial^2 \varphi}{\partial x^2} = \frac{e}{m}(n_e - n_0), \quad (3)$$

where A is the only non vanishing transverse component of vector potential $\vec{A} = (0, A, 0)$ under a Coulomb calibration, φ is the electrostatic potential, c is the speed of light, x the spatial coordinate (propagation direction), t is the time, v_x is the velocity in the parallel direction and n_0 is the initial number density of electrons. In the Vlasov equation the velocity in the perpendicular direction was replaced by the mean oscillatory velocity in the field of incident laser light $v_y = eA/m$. It means that in the perpendicular direction a monokinetic fluid description is considered [3]. The simplified Fokker-Planck collision term on the right hand side of the Vlasov equation, where ν_c is the effective collision frequency, is added. In the simulation, a realistic value of the collision frequency valid in the PALS experiment is used and it provides a satisfactory numerical stabilization of the method. For the normalization of the electron distribution function f we assume

$$\frac{n_e}{n_0} = \int_{-\infty}^{\infty} f \, dv, \quad (4)$$

by which the above system is closed. For the solution the unknown variables are rewritten as a sum of perturbed and unperturbed parts and a transformation method is used based on the Fourier-Hermite expansion of the distribution function, [4]. An adequate number of terms of Hermite series (700) and Fourier series (100) is used to reach a satisfactory accuracy of computations. We consider a homogeneous periodic plasma with the period L which is initially in a local statistical equilibrium. The finite spatial periodicity leads to the existence of the smallest wave number in the model $k_0 = 2\pi/L$, which determines the accuracy of the computation. The spatial period is chosen in such a way as to fulfill the wave vector matching condition within the discrete spectrum. The perturbed part of density was set equal to a low level white noise as a natural initial condition. A detailed description of the solution method and discussion of its numerical stability was a subject of an earlier paper [5].

The computations were performed using the following parameters, corresponding to a tight focus of the PALS experiment.

Parameter	Value
I_{Las}[1]	$1 \cdot 10^{20}$ W/m^2
λ_{vac}[2]	$1.3152 \ \mu$m
ω_L[3]	$1.432 \cdot 10^{15}$ s^{-1}
τ[4]	0.4 ns
T_e	$1 \cdot 10^7$ K
n_e/n_{cr}	0.044
n_e	$7.857 \cdot 10^{25}$ m^{-3}
ω_{pe}	$3 \cdot 10^{14}$ s^{-1}

3. Computational results

The temporal development of the electron distribution function is shown in Fig. 1. On the upstream side of the potential wave troughs modulating the electron distribution first in a non-resonant way a formation of phase space ellipses is clearly visible near the phase velocity of the electrostatic daughter wave, which are moving in the forward direction of the primary laser heating wave and is generated by the Raman backscattering. Ellipses in the phase space mean an oscillatory motion of the resonant electrons, which are trapped in the potential troughs of the forward moving electrostatic wave and perform a wobbling motion in the potential minima. This lasts till the back-scattered Raman electromagnetic wave grows strong enough to undergo a secondary Raman scattering itself, giving birth to a secondary electrostatic wave, which is this time moving in the backward direction. The backward moving electrostatic wave is, however, in turn capable of trapping electrons on the side of negative velocities of electron distribution function. If we wait

---

[1]Power density of pumping laser
[2]Vacuum laser wavelength
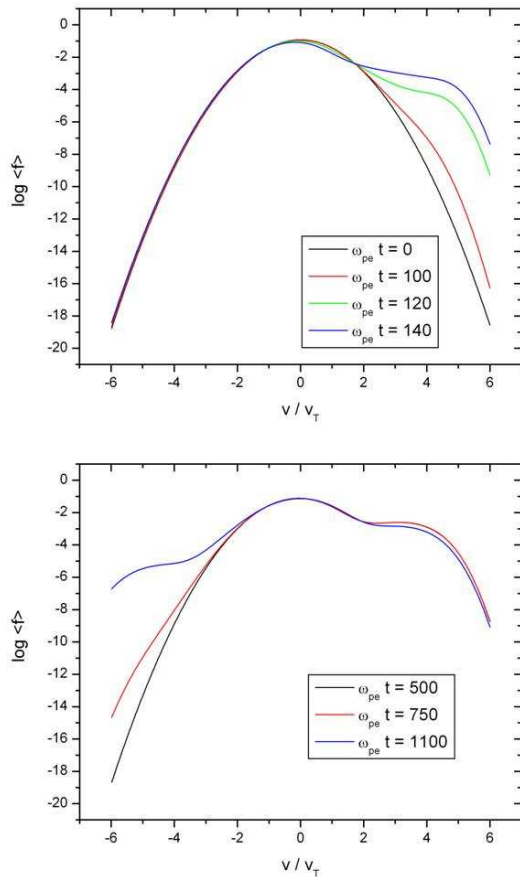[3]Laser frequency
[4]Pulse duration

Figure 2: Formation of plateau in vicinity of SRS-B plasma wave phase velocity is demonstrated by (a), where the spatially averaged electron distribution function over the simulation box at $\omega_{pe}t = 0, 100, 120$ and 140 is shown. Hot electron generation by SRS cascade is demonstrated by (b). Spatially averaged electron distribution is depicted there at $\omega_{pe}t = 500, 750$ and 1000. Note the logarithmic scale.

long enough (in real time about 5 ps for the parameters of the PALS laser) there is a reversal in the sense of motion of the perturbation on the negative velocity side, where initially the non-resonant modulation due to the primary wave is moving forward, till a resonant interaction caused by the secondary wave takes over and the direction is reversed. This is a demonstration of Raman cascading. The spatially averaged distribution function includes thus two plateaus - one each side. The more pronounced one on the positive velocity side corresponds to the primary Raman backscattering, the one on the opposite side is due to the Raman cascade, Fig. 2.

4. Discussion
This straight forward interpretation of the computational results is possible if the wave vector spectrum admissible in the expansions is only sparsely distributed, so as not to allow for a formation of the sidebands of the electrostatic daughter wave. The picture becomes more complicated if a denser wave vector spectrum is used and a formation of the sidebands becomes possible. In the advance stage of particle trapping it turns out that the trapped particles with the dynamics of their own behave as a "new" particle species giving rise to a new unstable mode leading to a growth of the sidebands. This new mode is a well known trapped particle instability recently discussed in [6]. As the sidebands grow, the trapping electrostatic field becomes more complex, the potential troughs of the trapping wave open and the trapped resonant electrons are freed. This, however, precludes the growth of the trapped particle instability and the sidebands disappear. The primary electrostatic wave starts to trap the electrons anew and the whole process is repeated. This means that in the computation a gros periodicity or an intermittency appears. The energy flow between the main electrostatic mode and the sidebands is asymmetric and invariably favours the lower sideband. We surmise that this should be interpreted as a nonlinear frequency lowering due to the finite amplitude effect of the primary wave.

References

[1] J. Lindel, Phys. of Plasmas 2 (1995) 3933.

[2] A. Sinquin, E. Lefebvre, Contributed papers, 32nd EPS Conference on Plasma Physics and 8th International Workshop on Fast Ignition of Fusion Targets, 2006.

[3] P. Bertrand, A. Ghizzo, S. J. Kartunen, T. J. H. Pattikangas, R. R. E. Salomaa, M. Shoucri, Phys. Plasmas 2, (1995) 3115.

[4] T. P. Armstrong, R. C. Harding, G. Knorr, D. Montgomery, "Methods in Computational Physics" vol. 9 (Academic Press 1970) 29.

[5] M. Mašek, K. Rohlena, Czech. J. Phys. 55 (2005) 973.

[6] S. Brunner, E. J. Valeo, Phys. Rev. Lett. 93 (2004) 145003.